

Duplex Steels: Part I: Genesis, Formation, Structure

Marina Knyazeva · Michael Pohl

Received: 19 December 2012 / Revised: 25 February 2013 / Accepted: 26 February 2013 / Published online: 9 April 2013
© Springer Science+Business Media New York and ASM International 2013

Abstract The ferritic–austenitic duplex steels are equipped with a mechanical–technological combination of properties, which is advantageous compared to the features of stainless completely ferritic or completely austenite steels. The duplex steels crystallize by fully ferritic or ferritic–austenite solidification with the austenite precipitation due to the solid solution reactions during the further cooling. To adjust the ferrite–austenite ratio, the steels must be heat treated by temperatures above the field of precipitation stability, followed by water quenching. The temperature and the time of the heat treatment effect the element distribution according to their higher solubility in the ferritic or austenitic phases. The typical microstructure of the duplex stainless steels can only be realized due to deformation and recrystallisation processing.

Keywords Microstructure · Steels · Metallography · Solidification · Properties

Introduction

Despite the fact that chromium, the main alloying element of the stainless steels, and its resistance to acid environments has been known since discovery of the element in 1797–1798, the history of corrosion-resistant steels does not begin until the end of the nineteenth century. The invention of the metal oxides reduction process with aluminum powder by Goldschmidt in 1895 made it possible to produce low-carbon ferrochrome. In 1910, Borchers and

Monnartz received a patent for the stainless steel manufacturing process. Monnartz was the first to explain the corrosion-resistant features of the chromium–iron compounds with the term “passivity” [1]. In 1912, the German Steel company KRUPP patented the austenitic steel types V2A (Cr, Ni) and V4A (Cr, Ni, Mo). The first article about the structure of austenitic stainless steels was published by Bain and Griffiths in 1927 [2].

Two-phase ferrite–austenite stainless steels have been studied since the late 1920s. In 1932, AVESTA Steelworks (Sweden) produced a ferrite–austenite material, which today is generally known as duplex steel. However, extensive use of this steel group only started in the 1980s, due to increasing demands from the chemical industry. Scarcity of nickel caused conventional austenitic steel to become very expensive.

Properties of the Duplex Steels

The properties of the ferrite–austenite steels combine high strength with high ductility and outstanding corrosion-resistant properties. The steels not only inherit the mechanical properties of the completely ferritic or completely austenitic alloys, but they also exceed them (Table 1). Examples of the three microstructures are shown in Fig. 1.

The advantages and disadvantages of duplex steels, compared to single-phased ferritic- and austenitic alloys, can be summarized as follows:

Advantages:

- Higher strength than austenitic steels
- Higher impact value than ferritic steels
- Increased resistance against general corrosion

M. Knyazeva · M. Pohl (✉)
Institute of Materials, Ruhr-Universität Bochum, Bochum,
Germany
e-mail: pohl@wp.rub.de

Table 1 Basic composition, and mechanical properties of three types of stainless steel

Structure	C	Cr	Ni	Short name	DIN	0.2 % YS Rp _{0.2} (MPa)	UTS Rp _m (MPa)	J (Av)	% E A ₅ (%)
Ferrite	<0.1	13–30	<1.0	X8Cr18	1.4015	345	540	–	20
Austenite	<0.1	17–26	7–26	X5CrNi18-10	1.4301	190	450	>100	45
Duplex	<0.1/0.4	24–28	4–7	X2CrNiMoN22-5-3	1.4462	450	700	>100	25

- Increased resistance against intergranular, pitting, crevice corrosion, and stress-corrosion cracking
- Higher resistance against hydrogen embrittlement than ferrites
- Better thermal conductivity than austenitic steels.

Disadvantages:

- Complex precipitation and transformation behavior
- High tendency to embrittlement due to formation of carbides, nitrides, and intermetallic phases
- Reduction of the corrosion resistance due to formation of carbides, nitrides, and intermetallic phases
- Advanced knowledge is needed for the production of components.

In 1969, to assess the corrosion resistance in chloride-containing media, Lorenz and Medawar [3] introduced the concept of chromium pitting resistance equivalent (PRE).

The most frequently used formula for PRE is

$$\text{PRE} = \text{Cr} + 3.3\text{Mo} + 16\text{N}$$

The stainless duplex steels are classified in relation to their corrosion resistance according to their PRE:

$$\text{Lean duplex} \leq 35 < \text{duplex} < 40 \leq \text{super duplex} < 45 \\ \leq \text{hyper duplex}$$

Development of PRE formulae from 1969 to 1995 is shown in Table 2.

Structure of Duplex Steels

The microstructure of duplex stainless steels is biphasic and consists of ferritic and austenitic components, both presented in approximately equal proportions in the material. The cast microstructure of duplex steels shows the precipitated austenitic phase within the ferritic matrix (Fig. 2). The phases in wrought duplex steel are arranged in pancake-like layers (Fig. 3).

A two-phase structure can be topologically characterized using volume ratio combined with phase distribution, and is divided into three structure types by Becker [4] as follows:

- I. Duplex
- II. Dispersion, and
- III. Net structure.

Dual-phase structures contain characteristics of the other three groups, and can be added to this range (see “IV” in Fig. 4). The crystal structure, which consists of (bcc) α and (fcc) γ , can be described by:

- Volume ratio,
- Density of the phase boundaries $L_S^{\alpha\gamma}$
- Density of the grain boundaries $L_S^{\alpha\alpha}$ or grain boundaries $L_S^{\gamma\gamma}$, respectively.

Characteristics of the two-phase materials can be calculated from the following parameters:

- Duplex-structures: Two structure components α and γ lie as crystals of the same size statistically distributed next to each other (volume ratio $V_V(\alpha) \approx V_V(\gamma) \approx 0.5$). Three types of boundary: α/α , γ/γ , and α/γ .
- Dispersion structure: All parts of the γ -phase lie isolated in the basic α -matrix (volume ratio $0 < V_V(\gamma) < 1$). Two types of boundary: α/α and α/γ .
- Net structure: The second phase (γ) precipitates only on the grain boundaries of the basic α -matrix (volume ratio $0 < V_V(\gamma) < 1$). Two types of boundary: γ/γ , and α/γ .
- Dual-phase structure: Similar to the duplex-structures the volume of the α - and γ -grains is equal and their distribution is regular and independent from the volume ratio. The γ -phase has to be isolated from α . At the same time, all grains of the second phase (γ) are only at grain boundaries. Two types of boundary: α/α and α/γ .

Although the typical pancake-like structure of the duplex steels with three types of boundary only occurs in wrought alloys, the name “duplex” has prevailed for cast structures as well; the latter is in fact a dispersion structure.

Ferritic–Austenitic Solidification

Adjustment of the two-phase microstructure of duplex stainless steels is complicated because a balanced phase ratio does not only depend on alloy components. The Schaeffler diagram, Fig. 5 [5], was originally developed for evaluation of weld structure resulting from non-equilibrium rapid cooling. It is based on the relation of the elements that stabilize the (bcc) or (fcc) lattice structures. Schaeffler’s original formula was modified by DeLong and

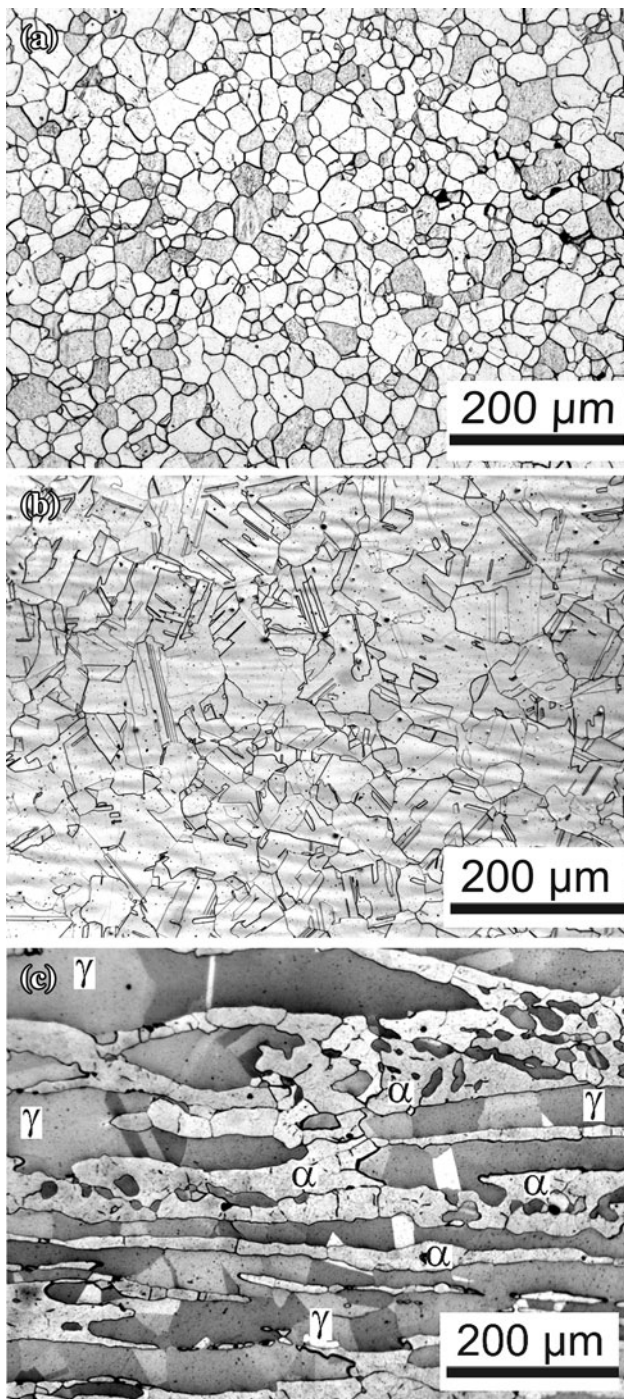


Fig. 1 Microstructural comparison of **a** ferritic, **b** austenitic, and **c** ferritic–austenitic duplex stainless steels. Etchant: aqua regia/V2A-pickle (ferrite, austenite) and Beraha II reagent (duplex)

other authors in the 1970s [6, 7]. A summary of modifications is provided in Table 3.

An increased content of alloying elements in steel will suppress the martensitic transformation and result in an austenitic (high Ni_{eq}) or a ferritic (high Cr_{eq}) structure. With a lower content of austenite-stabilizing elements, a

Table 2 Development of pitting resistance equivalent (PRE) since 1969

Source	PRE
Lorenz (1969)	% Cr + 3.3 % Mo
Truman (1978)	% Cr + 3.3 % Mo + 16 % N
Herbsleb (1982)	% Cr + 3.3 % Mo + 30 % N
Gysel (1987)	% Cr + 3.3 % Mo + 1 % N
Heimgartner (1988)	% Cr + 3.3 % Mo + 15 % N + 2 % Cu
Rondelli (1995)	% Cr + 3.3 % Mo + 30 % N – 1 % Mn

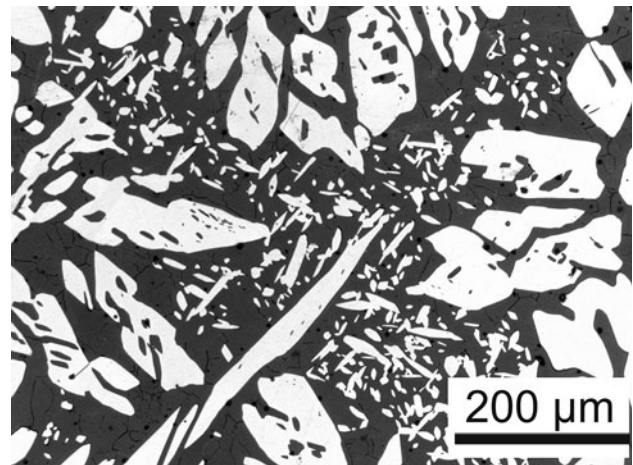


Fig. 2 Typical distribution of austenitic (*white phase*) and ferritic (*black phase*) phases in a cast duplex stainless steel. Etchant: Beraha II reagent

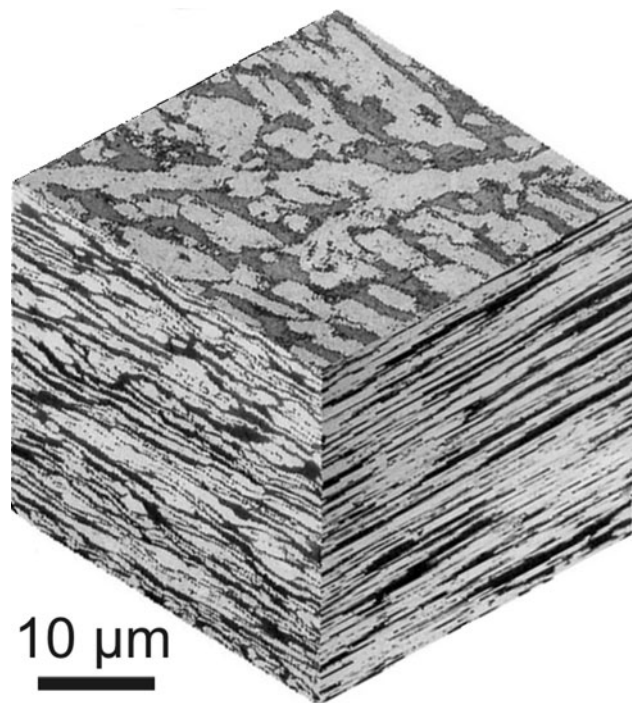


Fig. 3 Structure of a rolled duplex stainless steel

Fig. 4 Four types of two-phase structures

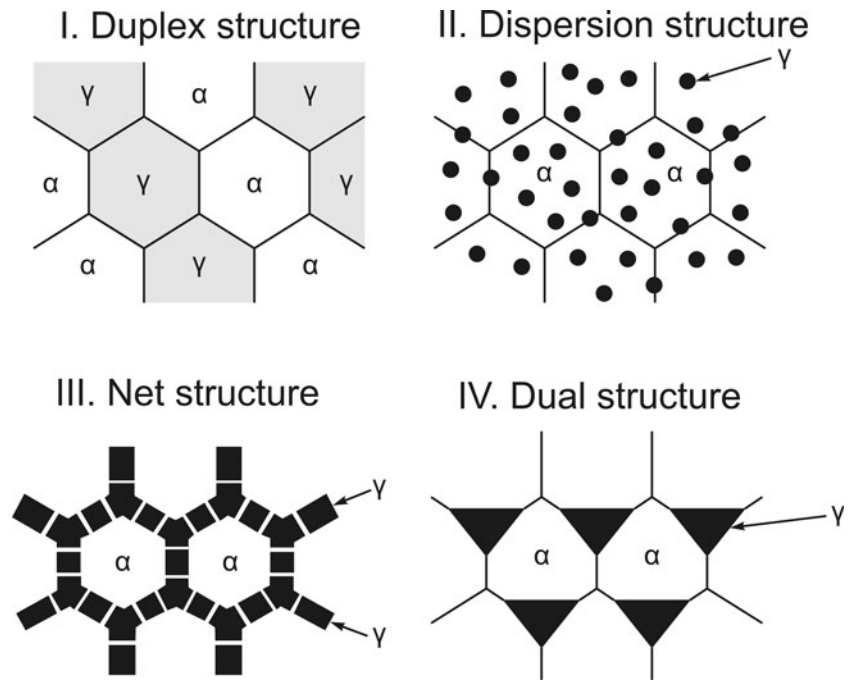
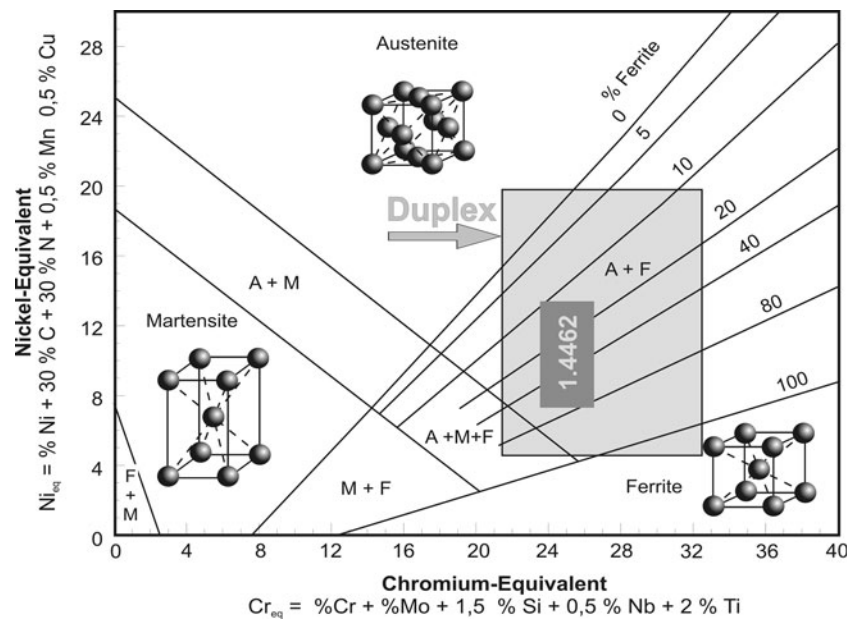


Fig. 5 Schaeffler–DeLong phase diagram [5]



ferritic–austenitic microstructure will be formed. Variations in the chemical composition of duplex stainless steels will lead to low reproducibility of the phase ratio, especially under conditions of uncontrolled cooling (Fig. 5).

The two-phase solidification can proceed in different ways, as illustrated in Fig. 6. The manner of solidification for these high-alloy steels depends primarily on their chemical composition. A thermodynamically based mathematical model [7] operates with an ϕ -value, which predicts the type of primary crystallization:

$$\phi = Ni_{eq} - 0.75Cr_{eq} + 0.257,$$

where

$$Ni_{eq} = Ni + 0.31Mn + 22C + 14.2N + Cu$$

$$Cr_{eq} = Cr + 1.37Mo + 1.5Si + 2Nb + 3Ti,$$

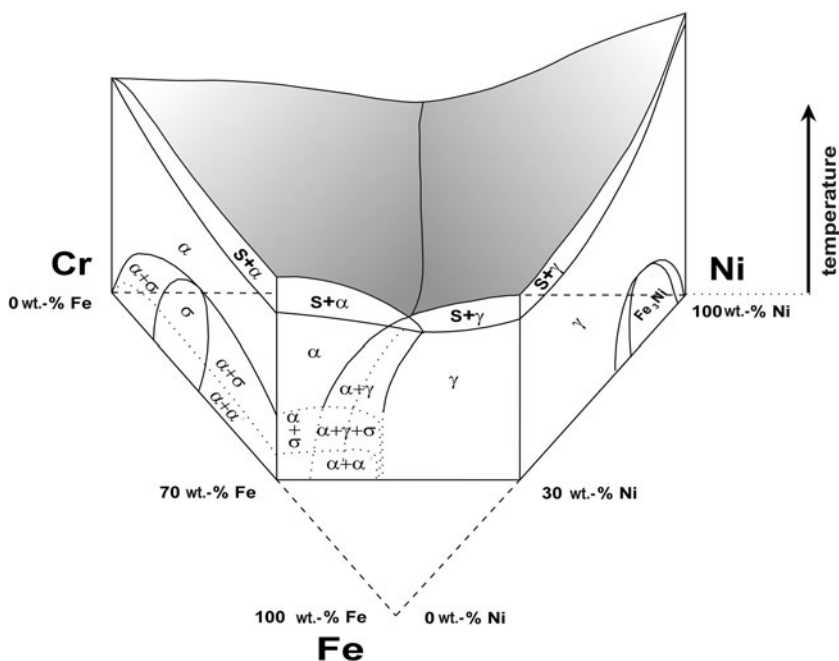
and

- $\phi \ll 0$: ferritic primary solidification
- $\phi \gg 0$: austenitic primary solidification
- $\phi \approx 0$: ferritic–austenitic solidification.

Table 3 Nickel- and chromium equivalents proposed by different authors

Source	Nickel equivalent
Schaeffler (1949)	% Ni + 30 % C + 0.5 % Mn
DeLong (1974)	% Ni + 30 % C + 0.5 % Mn + 30 % N
Hammar (1979)	% Ni + 22 % C + 0.31 % Mn + 14.2 % N + % Cu
Source	Chromium equivalent
Schaeffler (1949)	% Cr + % Mo + 1.5 % Si + 0.5 % Nb
Hammar (1979)	% Cr + 1.37 % Mo + 1.5 % Si + 2 % Nb + 3 % Ti
Berns (2008)	% Cr + 1.4 % Mo + 1.5 % Si + 0.5 % Nb + 2 % Ti

Fig. 6 Quasi-binary section through the Fe–Cr–Ni diagram at 70 % iron



With duplex steels, it is necessary to distinguish between two different solidification processes. A quasi-binary section through the Fe–Cr–Ni diagram at 70 % iron shows a simplified image of the range of existence of duplex steels (Fig. 7).

Solidification of duplex steels is controlled by chemical composition. If the percentage of ferrite formers is high, the material will solidify at the chromium-rich side of the eutectic field, with the formation of α -crystals $S \rightarrow \alpha$. Initially, the solidification is completely ferritic. On further cooling, a diffusion-controlled solid-state reaction $\alpha \rightarrow \alpha + \gamma$ takes place, resulting in inter- and intragranular precipitation of the austenitic phase.

The second possible route is a so-called flip-flop solidification, which occurs close to the eutectic valley at a very slow cooling rate and with an increased amount of austenite-stabilizing elements (especially C and N). In this case, solidification begins with primary ferrite

crystallization from the liquid phase. The melt is hence depleted of ferrite-stabilizing elements (e.g., Cr and Mo) and the concentration of austenite stabilizers (Ni, Cu, Mn, C, and N) increases. Equilibrium is thus shifted in the three-phase valley $S + \alpha + \gamma$, which promotes formation of the γ -solid solution crystals. Formation of austenite leads to melt depletion of the austenite stabilizers and so ferrite solidification is again favored.

This interchangeable crystallization is actually a simultaneous solidification of α -dendrites and interdendritic γ -crystals, repeating until the solidification is completed. Cooling further down, the austenite ratio increases due to diffusion-driven growth of the γ -crystals, or also due to diffusion-controlled solid solution transformation $\alpha \rightarrow \alpha + \gamma$. These two types of austenite are distinguished in Fig. 8b. The austenite emerging “primarily” from the molten metal as a result of the flip-flop crystallization is indicated as γ_1 . The “secondary” austenite,

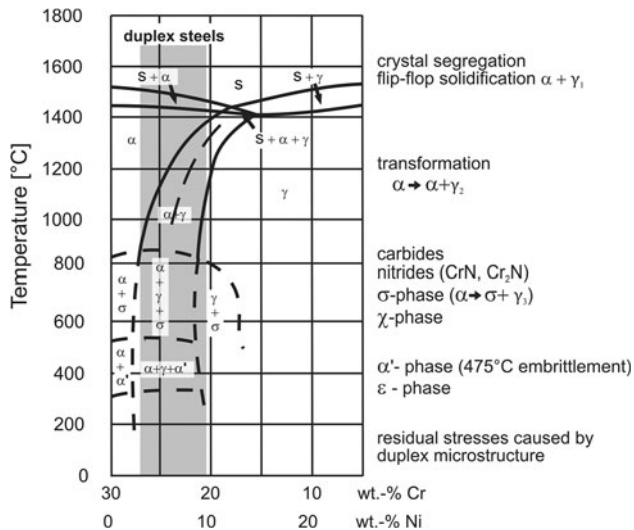


Fig. 7 Quasi-binary section through the Fe–Cr–Ni diagram at 70 % iron. Range of existence of duplex steels (*gray*) and overview of phase formation

γ_2 , is formed by solid solution transformation from the ferritic phase.

During rapid cooling, and especially at low temperatures, a solid-state transformation of the ferrite into an austenite structure is possible due to a nearly diffusionless transformation, which shows similarities to martensite formation. In this case, Ohmori et al. [8] describe a “shear-supported diffusion” mechanism. The secondary austenite formed in this way has a similar composition to the ferritic matrix. The tertiary austenite γ_3 arises below 1,000 °C as a result of ferrite decomposition due to eutectoid solid-state reaction (for example, $\alpha \rightarrow \sigma + \gamma_3$).

Melt solidification and austenite formation proceed according to thermodynamic laws and the mechanisms of nucleation and growth. The driving force for nuclei formation arises from supercooling of the melt to a lower critical temperature ΔT ; this usually occurs at the mold wall. The stronger the supercooling, the more nuclei appear; they grow slowly due to suppressed substitutional diffusion. A slight supercooling leads to the formation of a few, but fast-growing nuclei. The austenite precipitates in the same way, regardless of whether it is primary or secondary austenite. The result is formation of a finer austenitic grain structure at low temperature, Fig. 8b. The austenite precipitation favors the Kurdjumov–Sachs orientation. Because the ferrite lattice 100-planes correspond with the lattice parameter of the 111-planes of the austenite, the austenite grows here. The resulting defect-free phase boundary provides good stress transition from ferrite to austenite and ensures good deformation properties. In this temperature range, a Widmannstätten structure occurs through the preferential growth of austenitic crystals in a $\langle 112 \rangle$ direction. The scientific literature also cites

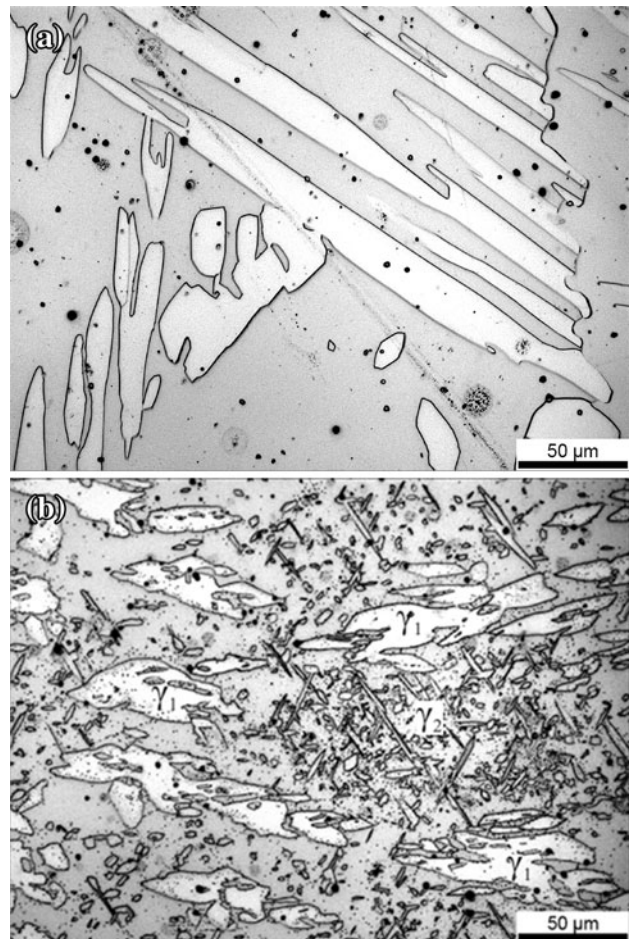


Fig. 8 Changes in austenite morphology (*white phase*) resulting from different temperatures of formation. **a** 1,200 °C, **b** 1,000 °C

orientations shown in Table 4 [9–12]. Cooling rate exerts a strong influence on the primary solidification: the higher the Cr_{eq}/Ni_{eq} ratio, the slower the cooling rate must be to promote a two-phase structure.

Although the boundary between the α and $\alpha + \gamma$ stability field shown in Fig. 7 remains nearly stable below 1,000 °C, the addition of further alloying elements changes the ferrite–austenite ratio according to the temperature. Figure 9 shows how the percentage of the austenite increases with decreasing temperature.

A 50:50 ferrite:austenite relationship is an ideal goal for duplex steel microstructure. In reality, however, the phase fractions cover a slightly wider range and are between 40:60 and 60:40. Equal proportions have proved to be ideal for mechanical and corrosion properties. This phase relation can be achieved exclusively by special heat treatment. The resulting microstructure ratio can be determined using magnetic, x-ray, or metallographic methods. It should be noted, however, that the different methods can lead to varying results, as demonstrated in Table 5 [13].

Table 4 Orientation relationships between ferrite and austenite

Orientation relationship	Lattice correspondence relation	Misorientation angle/axis
Bain [9]	$\{001\}\gamma//\{001\}\alpha$ $\langle 110\rangle\gamma//\langle 110\rangle\alpha$	$45^\circ/\langle 001\rangle$
Kurdjumov–Sachs (K–S) [10]	$\{111\}\gamma//\{011\}\alpha$ $\langle 011\rangle\gamma//\langle 111\rangle\alpha$	$42.8^\circ/\langle 2\ 11\rangle$
Nishiyama–Wassermann (N–W) [11, 12]	$\{111\}\gamma//\{011\}\alpha$ $\langle 112\rangle\gamma//\langle 011\rangle\alpha$	$45.9^\circ/\langle 254\rangle$

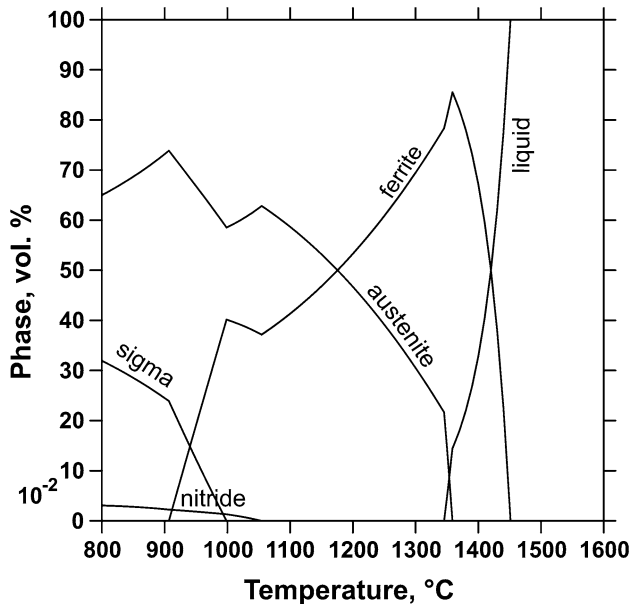


Fig. 9 Phase ratio–*T* diagram for the system 22Cr–5Ni–3Mo–0.2N (DIN 1.4462)

Even though solidification and phase transformation of duplex stainless steels are complicated, non-equilibrium processes, a numerical simulation is feasible by optimizing the thermodynamically based databases such as *ThermoCalc* and *Dictra* from the Swedish Royal Institute of Technology, Sweden [14].

Heat Treatment and Distribution of the Alloying Elements

The phase ratio and a homogenized, precipitation-free microstructure can be adjusted by a solution annealing heat treatment. This type of heat treatment is carried out at temperatures above 1,000 °C and must be completed by quenching in water as rapidly as possible.

The system is thermodynamically unstable because of the high fraction of alloying elements. During cooling

Table 5 Comparison of different experimental measuring methods [13]

Material	Ferrite (vol%) Heat treatment: 1,050 °C/2 h/water quenching		
	Quantitative image analysis	Magnetic inductive testing	x-ray diffraction
X2CrNiMoN 22-5-3	48	44	47
GX4CrNiMoN 27-5-2	70	72	64
GX3CrNiMoCuN 26-6-3-3	40	32	35
GX40CrNiMo 27-5	40	40	45

Table 6 Maximum solubility of alloying elements in α and γ iron (wt%) [15]

Element	Lattice structure	α -Iron	γ -Iron
W	bcc	35	4.7
Mo	bcc	31	1.7
Mn	fcc	3.5	100
Cr	bcc	100	12.5
Cu	fcc	2.1	12
Ni	fcc	6	100
Si	Diamond lattice	11	1.7
C	–	0.03	2.1
N	–	0.1	2.8

below 1,000 °C, the formation of a variety of other, often undesirable, phases occurs. To ensure a precipitation-free microstructure, the material must be quenched from a temperature above the formation (from solid solution) of carbides, nitrides, and intermetallic phases. Due to the different solid solubility potential for alloying elements in the bcc and fcc lattices, especially for interstitial atoms, the ferritic and austenitic phases have different chemical compositions. The distribution of alloying elements is not only dependent on the respective solubility limits of elements (Table 6 [15]) but is also influenced by heat treatment temperature and duration, and by cooling rate.

Due to octahedral and tetrahedral interstitial sites within the crystal lattice, elements such as C and N have as much as two orders of magnitude higher solubility in the fcc lattice, and therefore are enriched in austenite. The distribution of other alloying elements follows the principle of the solubilities shown in Table 6, and is more significant the lower the temperature and the longer the heat treatment time. The interstitial elements C and N, and the fcc lattice stabilizing elements such as Ni, Cu, and Mn concentrate in

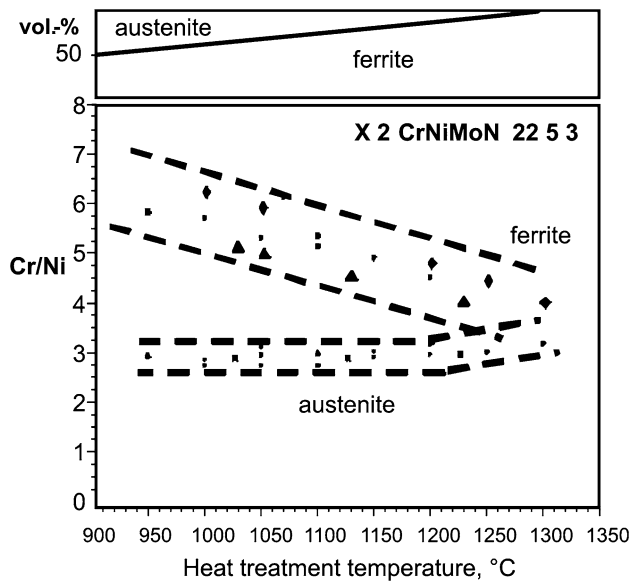


Fig. 10 Phase fraction (vol%) and Cr/Ni-ratio as a function of heat treatment temperature [16]

the austenite phase, while ferrite is enriched with Mo, Cr, and W.

Figure 10 shows the variation of the Cr/Ni-ratio in ferrite and austenite depending on heat treatment temperature. During formation and growth, the freshly generated austenite exhausts the fcc-stabilizing elements such as Ni and Cu from ferrite, due to their movement by diffusion to the fcc lattice. The ferrite therefore becomes enriched in Cr and Mo, and results in an increase of the Cr/Ni-ratio. The volume fraction of ferrite decreases at lower heat treatment temperature. As the cooling rate is a “heat treatment” with continuously decreasing temperature, the slow cooling also promotes significant element segregation.

Microstructure and Grain Size

As described earlier, in cast alloys, the grain size increases with the decreasing sub-cooling and reduced cooling rate. In his study, Wischnowski performed multistage heat treatments to achieve refinement of the austenite. No measurable impact on 0.2 % yield stress was detected and only a slight increase in tensile strength was observed [16].

Deformation and subsequent recrystallization causes grain refinement. In this way, duplex steels obtain their typical pancake-like structure, resulting in a large increase in strength and toughness according to the Hall–Petch principle. The two-phase microstructure inhibits grain growth during deformation and heat treatment. While the austenite phase coarsens slowly, the grains of the ferritic phase tend to coalesce because of the rapid diffusion processes in the bcc lattice (Fig. 11).

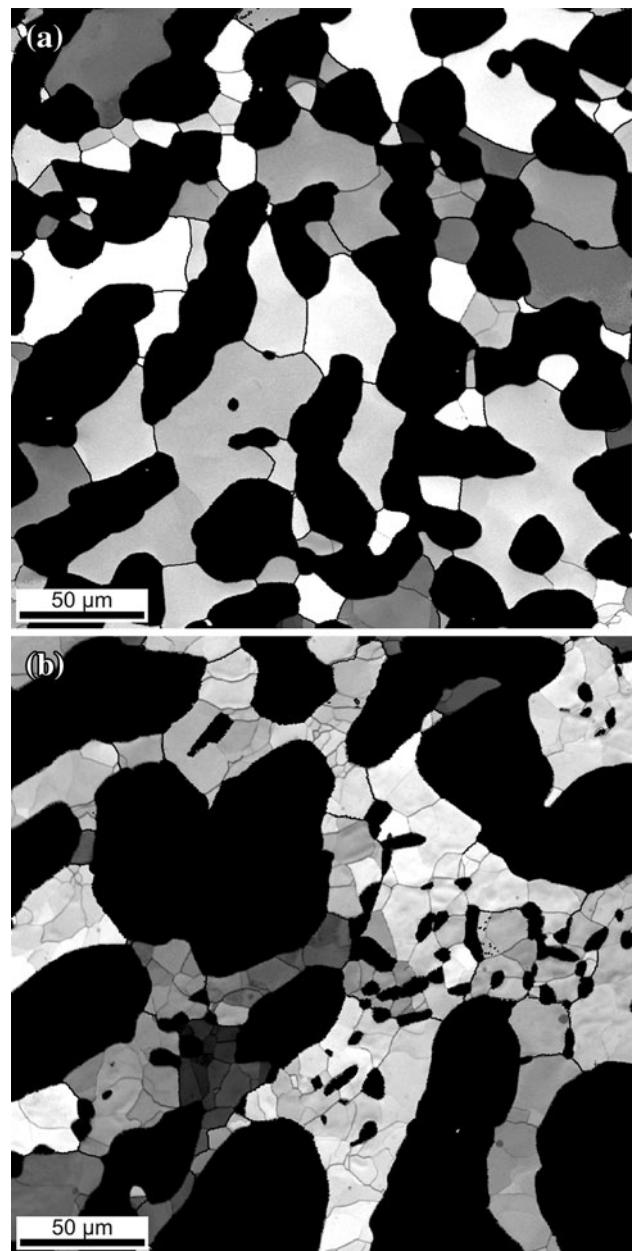


Fig. 11 Coalescence of the ferritic grains (*gray phase*) and coarsening of austenitic grains (*black*) during heat treatment. **a** Ferrite grains after short heat treatment time. **b** Ferrite grains after long heat treatment time. EBSD images

Summary

The ferritic–austenitic duplex steels exhibit a range of properties, based on thermo-mechanical treatments, which are advantageous when compared to the features of completely ferritic or completely austenite stainless steels. The duplex steels crystallize as fully ferritic or ferritic–austenite solidification, with austenite precipitation resulting from solid solution reactions during further cooling. To adjust the ferrite–austenite ratio, the steels must be heat treated

above the temperature of second phase formation, and this must be followed by rapid quenching. The temperature and time of heat treatment affect element distribution according to their solubility in the ferritic or austenitic phases. The typical microstructure of duplex stainless steels can only be realized through a combination of mechanical working (deformation) and recrystallization processing.

References

1. P. Monnartz, *Contribution to the study of iron–chromium alloys with special attention to their acid resistance*. Dissertation, Königliche Technische Hochschule, Aachen, 1911
2. E.C. Bain, W.E. Griffiths, An Introduction to iron–chromium–nickel alloys. *Trans. Am. Inst. Min. Metall. Eng.* **75**, 166–211 (1927)
3. K. Lorenz, G. Medawar, About the corrosion behaviour of Cr–Ni–Mo austenitic steels with and without nitrogen addition taking their resistance in chloride solutions. *Thyssen Research* **1**(3), 97–108 (1969)
4. J. Becker, E. Hornbogen, P. Stratmann, Dual-phase structures. *Int. J. Mater. Res.* **71**(1), 27–31 (1980)
5. A.L. Schaeffler, Constitution diagram for stainless steel weld metal. *Met. Prog.* **56**(5), 680A & 680B, 1949
6. W.T. DeLong, Ferrite in austenitic stainless steel weld metal. *Weld. J.* **53**(7), 273s–286s (1974)
7. O. Hammar, U. Svensson, Influence of steel composition on segregation and microstructure during solidification of austenitic stainless steels, in *Solidification and Casting of Metals* (London, The Metals Society, 1979), pp 401–410
8. Y. Ohmori, K. Nakai, H. Ohtsubo, Y. Isshiki, Mechanism of Widmannstätten austenite formation in a α/γ -duplex phase stainless steel. *ISIJ Int.* **35**(8), 969–975 (1995)
9. E.C. Bain, The nature of martensite. *Trans. AIME* **70**, 25 (1924)
10. G. Kurdjumov, G.Z. Sachs, About the mechanism of steel hardening. *Physik* **64**, 325 (1930)
11. Z. Nishiyama, X-ray investigation of the mechanism of the transformation from face-centred cubic lattice to body-centred cubic. *Sci. Rep. Tôhoku Imp. Univ. Tokio* **23**, 637 (1934)
12. G. Wassermann, K. Mitt, About the mechanism of α - γ transformation of the iron. *Wilh.-Inst. Eisenforsch.* **17**, 149 (1935)
13. M. Pohl, The ferrite–austenite ratio of duplex-stainless steels. *Z. Metallkunde* **86**(2), 97–102 (1995)
14. M. Mola: *Numerical development of ferritic–austenitic duplex steels with reduced nickel content*. Dissertation, Ruhr-Universität, Bochum, 2005
15. H. Berns, W. Theisen, in *Ferrous Materials—Steel and Cast Iron* (Springer, Berlin, 2008), pp. 47 & 322
16. F. Wischnowski, *Effect of microstructural modifications on the corrosion resistance of stainless ferritic–austenitic duplex steels*. Dissertation, Ruhr-Universität, Bochum, 1995